ISSN 0965-545X, Polymer Science, Ser. A, 2014, Vol. 56, No. 6, pp. 936–944. © Pleiades Publishing, Ltd., 2014.

THEORY AND SIMULATION

Monte Carlo Simulation Study of the Effect of Chain Tacticity on Demixing of Polyethylene/Polypropylene Blends[1]

Adisak Takhulee and Visit Vao-Soongnern

Laboratory of Computational and Applied Polymer Science, School of Chemistry, Institute of Science, Suranaree University of Technology, Nakhon Ratchasima 30000, Thailand

e-mail: D5010486@g.sut.ac.th, visit@sut.ac.th

Received April 10, 2014;
Revised Manuscript Received August 1, 2014

Abstract—The molecular origin of the demixing behavior for 50 : 50 (wt/wt) polyethylene/polypropylene (PE/PP) with different tacticity of PP at the melts (473 K) was investigated by Monte Carlo simulation of coarse-grained polymer model. *Isotactic* (*i*PP), *atactic* (*a*PP) and *syndiotactic* (*s*PP) polypropylenes were used for blending with PE. Coarse-graining polymer chains were represented by 50 beads, corresponding to $C_{100}H_{202}$ and $C_{150}H_{302}$ for PE and PP, respectively. The simulation was performed on a high coordination lattice incorporating short-range intramolecular interactions from the Rotational Isomeric State (RIS) model and long-range intermolecular interactions Lennard–Jones (LJ) potential function of ethane and propane units. Chain dimensions, the characteristic ratio (C_n) and self-diffusion coefficient (D) of PE in the blends are sensitive to the stereochemistry of PP chains. Compared with neat PE melts, PE dimension was relatively unchanged in PE/*i*PP and PE/*a*PP blends but slightly decreased in PE/*s*PP blends. PP dimension was increased in PE/*i*PP and PE/*a*PP mixture but decreased in PE/*s*PP blend in comparison with neat PP melts. In addition, diffusion of PE and PP chains in PE/PP mixture was decreased and increased, respectively, compared to the pure melts. Interchain pair correlation functions were used to detect the immiscibility of the blends. The tendency of demixing of PE/*a*PP and PE/*i*PP blends were weaker than that of PE/*s*PP blend.

DOI: 10.1134/S0965545X14060200

INTRODUCTION

Blending is one of the most effective methods to develop new polymeric materials for special application by mixing two or more components together. The usual objective for preparing a novel blend is not to change the properties of the components drastically but to capitalize on the maximum possible performance of the blend. The physical properties of the polymer blends depend on the miscibility of each component [1].

Due to the chemical similarity of their structural groups, many polyolefin melts have very similar physical properties, including density–temperature relationships and optical characteristics such as the refractive index, making some analytical techniques inappropriate for the detection of phase separation. Thermodynamic interactions in polyolefin blends are very weak and have been shown to originate from induced-dipole forces, but they differ in subtle, depending on the component structures [1–3]. A lack of a single dominant thermodynamic factor determining phase behavior allows polyolefin blends to be influenced by subtle variations in molecular architecture [4].

Polyolefin blend behavior is also difficult to study theoretically because the thermodynamics is determined by subtle differences in the structure of the different polymer components. The effects of these differences are amplified by the large number of monomers in a single polymer chain to the point where even isomers of the same type of polymer become immiscible for large chains. Molecular packing may be the dominant influence on polyolefin miscibility, so the accurate prediction of the polyolefin melt structure would enable some of the reasons for the difficulty of miscibility prediction to be studied. In the melt, molecules of a homopolymer polyolefin, such as linear PE or PP, generally exist in random conformations, but some order is present because of weak intramolecular and intermolecular interactions. Molecular conformation, governed by the configuration of the functional groups, influences the packing of the polymer chains, determining the melt structure, density, and the miscibility of polyolefins in the melt state. The physical properties of the melt are also then largely determined by conformation. The presence of side groups is also influent on polymer conformation and packing. An understanding of the polyolefin melt structure and miscibility will enable a scientific approach to blending in which components are chosen

[1] The article is published in the original.

Table 1. Simulation details for PE, PP and PE/PP systems

System	Number of polymer chains				Density, g cm^{-3}
	PE	*a*PP	*i*PP	*s*PP	
PE	29	–	–	–	0.760
*a*PP	–	19	–	–	0.750
*i*PP	–	–	19	–	0.750
*s*PP	–	–	–	19	0.750
PE/*a*PP	14	9	–	–	0.756
PE/*i*PP	14	–	9	–	0.756
PE/sPP	14	–	–	9	0.756

to enhance specific properties within the blend over the components [5–8].

In addition to experimental and theoretical approaches, Molecular Dynamics (MD) [7] and Monte Carlo (MC) [8] simulations are the most accurate computational approaches for studying polymer blends because, for a given molecular model, simulation gives exact results for the statistical thermodynamics of mixing. Unfortunately, it is not feasible to mix blends of large chain lengths to follow the phase separation. Small changes in the covalent structure of polymeric hydrocarbon chains can easily produce immiscibility of their high polymers, even though miscibility may be retained with mixtures of small oligomers [9]. Melts composed of two different polymeric hydrocarbons provide numerous examples. This show that hydrocarbon polymer is sensitive to structural changes which make the miscibility of polyolefins in the melt is difficult to predict. Therefore, two-component systems composed of pairs of hydrocarbon homopolymers are the subject of intense both experimental and theoretical studies. For examples, the mixtures of *atactic* polypropylene (*a*PP) and isotactic polypropylene (*i*PP) are observed to be miscible, but replacement of either component with syndiotactic polypropylene (*s*PP) induces phase separation in the melt [8–10].

Here, Monte Carlo simulation of coarse-grained polymer model from previous studies of PP/PP blends with different stereochemistry [8–10] is employed to investigate PE/*i*PP, PE/*a*PP and PE/*s*PP blend melt in addition to past theoretical and MD studies of PE/*i*PP reported in literatures [6, 7]. It would be interesting to employ simulation in addition to experiment as most of PE samples always contain some sort of branching. The main objective of this simulation work is to gain more understanding for the molecular origin of the dependence of the demixing behavior for 50 : 50 (wt/wt) PE/PP with different tacticity of polypropylene at the melts.

SIMULATION SETUP

The Second Nearest Neighbor Diamond (2nnd) Lattice

PE and PP were modeled by a chain of beads represented by $-CH_2CH_2-$ and $-CH_2CH(CH_3)-$ unit, respectively. The coarse-grained beads were represented by two backbone carbons, which can be placed on the second nearest neighbor diamond (2*nnd*) lattice. This 2*nnd* lattice was constructed by removing all second alternating sites from the tetrahedral diamond lattice. The lattice has $10i^2 + 2$ sites in the i^{th} shell, identical to the closest packing of hard spheres. The unit cell is represented as a distorted cube. The distance between any two connected sites, i.e., the step length (L) can be determined from the step length of the underlying diamond lattice (l) by $L = 2\sqrt{2/3}\,l$. For the simulation of the PE and PP melts, $l = 0.153$ nm, therefore $L = 0.250$ nm. The occupancy of the 2*nnd* lattice is quite low even at bulk conditions since each occupied site represents two backbone atoms. For examples, for bulk PE with density = 0.76 g cm^{-3} at 473 K, the occupancy is 18%. The density for PP is lower (12% for a density = 0.75 g cm^{-3} at 473 K) [8–11].

Simulation Systems

Homopolymer of PE, *a*PP, *i*PP and *s*PP and the binary blend of 50/50 (wt/wt) PE/*a*PP, PE/*i*PP and PE/*s*PP were simulated at 473 K. Independent coarse-grained chains of $C_{100}H_{202}$ (PE) and $C_{150}H_{302}$ (PP) were built in the periodic boundary condition The box size is $20 \times 20 \times 20$ unit cell which is equivalent to $50 \times 50 \times 50$ Å^3 (about 3.5 Rg$^{1/2}$ of polymer chains to reduce the finite size effect). Each chains consist of 50 beads which represent $H-(CH_2CH_2)_{100}-H$ and $H-(CH_2CH(CH_3))_{100}-H$ for PE and PP, respectively. This chain length is below the entanglement length but long enough to investigate the conformation and packing characteristics that influence the demixing behavior of PE/PP blends. The fraction of sites occupied for pure PE and PP melts are 0.181 and 0.119, correspond to the density of 0.760 and 0.750 g cm^{-3}, respectively [12]. PE and PP of 29 and 19 chains, respectively, were performed in the simulation for neat melt. The PE/PP melt blends were composed of 14 PE and 9 PP chains (occupancy = 14.6% and density = 0.756 g cm^{-3}). The blend density is taken as the arithmetic average of the value for its pure components. The summarized information for the simulation is presented in Table 1.

Hamiltonian

The interaction energies in this model contains two parts. The rotational isomeric state (RIS) models [13, 14] used for the intramolecular short-range interactions were the classic model described for PE [15] and

PP [16]. The RIS model by Suter et al. [16] was used for PP, which had three short-range interactions, with statistical weights denoted by η, τ, and ω. Two successive bonds of *meso* diad in *i*PP contributed to the conformational partition function via the product of the two statistical weight matrices as following:

$$\begin{bmatrix} \eta & 1 & \tau \\ \eta & 1 & \tau\omega \\ \eta & \omega & \tau \end{bmatrix} \begin{bmatrix} \eta\omega & \tau\omega & 1 \\ \eta & \tau\omega & \omega \\ \eta\omega & \tau\omega^2 & \omega \end{bmatrix} \quad (1)$$

In case of *s*PP, four successive bonds in *s*PP chains contributed via the product of four statistical weight matrices

$$\begin{bmatrix} \eta & 1 & \tau \\ \eta & 1 & \tau\omega \\ \eta & \omega & \tau \end{bmatrix} \begin{bmatrix} \eta & \omega & \tau\omega \\ \eta\omega & 1 & \tau\omega \\ \eta\omega & \omega & \tau\omega^2 \end{bmatrix} \begin{bmatrix} \eta & \tau & 1 \\ \eta & \tau & \omega \\ \eta & \tau\omega & 1 \end{bmatrix} \times \begin{bmatrix} \eta & \tau\omega & \omega \\ \eta\omega & \tau\omega^2 & \omega \\ \eta\omega & \tau\omega & 1 \end{bmatrix} \quad (2)$$

*a*PP was described by the statistical weight matrices defined along with

$$\begin{bmatrix} \eta\omega & 1 & \tau\omega \\ \eta\omega & \omega & \tau\omega^2 \\ \eta & \omega & \tau\omega \end{bmatrix} \quad (3)$$

These statistical weights were formulated as Boltzmann factors with energies $E_\eta = 0.29$ kJ/mol, $E_\tau = 3.8$ kJ/mol, and $E_\omega = 8.0$ kJ/mol. The description with a 3×3 statistical weight matrix was mapped into a precisely equivalent model for each $-CH_2CH(CH_3)-$ unit. The probability for any PP chain conformation of specified stereochemical sequence can be deduced from the 9×9 statistical weight matrices by using the RIS model techniques [9, 21].

The long-range interaction in the pure polymer melts were treated with a discretized Lennard-Jones (LJ) potential energy [17] that describe the pairwise interactions of ethylene ($\varepsilon_{PE,PE}/k_B = 205.0$ K, $\sigma_{PE,PE} = 4.2$ Å) and propane ($\varepsilon_{PP,PP}/k_B = 237.1$ K, $\sigma_{PP,PP} = 5.1$ Å) [18]. For interaction between the beads in PE/PP mixture ($\varepsilon_{PE,PP}/k_B = 220.5$ K, $\sigma_{PP,PP} = 5.7$ Å), were obtained by the Berthelot mixing rules [12]. At the temperature of the simulations, 473 K, discretization of these LJ potential energy functions produces the first three shell energies as: PE–PE interaction (12.980, 0.101, –0.593 kJ/mol); PP–PP interaction (26.693, 3.065, –1.088 kJ/mol) and PE–PP interaction (18.401, 1.178, –0.879 kJ/mol). A large positive value is obtained for the first shell because it covers distances smaller than σ. The value of the second shell is also positive and the strongest attraction is found in the third shell.

Moves

Two types of local moves were used during the simulation. One type is the set of single-bead moves. These moves correspond to three- or four-bond crankshaft motions in atomistically detailed description of the chain. The other type is a set of multiple-bead local moves based on the pivot algorithm methodology [19]. The specific set used in this simulation applies an appropriate symmetry operation to a subchain consisting of 2, 3, or 4 consecutive beads in a coarse-grained chain. Incorporation of the multiple-bead moves significantly improved the rate of equilibration of the PP melt. The moves avoided double occupancy of any site and also rigorously avoided the "collapse" of beads. Acceptance of a proposed move was based on the Metropolis criteria [20] at 473 K, where the ΔE is the sum of the changes in the local intrachain (rotational isomeric state) and interchain non-bonded interactions.

After the initial structure was created, an equilibration run was performed at least 10 million Monte Carlo steps (MCS). Each MCS is defined as an attempt to move each bead in the system once. Once the system reached equilibrium, production run of additional 10 million MCS were performed. To improve the statistics, three independent runs from different initial structures were performed. The reported properties in this work were the ensemble averaged from these independent runs. To study the dynamic properties, only the single bead move was employed after the equilibration step.

RESULTS AND DISCUSSION

Equilibration

The criterion to assess equilibration in each system is that the mean distance moved by the chains is greater than $2R_g$. The typical mean square displacements (MSD) of the center of mass (g_3), for example, PE and *a*PP chains of in neat melts and in PE/*a*PP blend are shown in Fig. 1a. The results show that the polymer chains moved greater than $2R_g$ within 10 million MCS. In addition, the orientation auto-correlation function (OACF) of the end-to-end vector was also calculated to ensure the equilibrated structure. As shown in Fig. 1b, OACFs of the end-to-end vector decay from an initial value to zero also within 10 million of MCS. The equilibrated structures for all except syndiotactic system were achieved within this simulation time. Syndiotactic melts decay at a considerably slower rate due to the higher preference for longer *trans* sequences resulting in a stiffer chain. Very long simulation time about 93.6×10^6 MCS is needed to fully equilibrate *s*PP system as estimated from MSD line to reach $2R_g$. To improve the statistics of our results, three independent runs from different initial structures were performed. The results used for analysis of PE/PP demixing were not significantly different from each set of data. Therefore, our simulation can provide reasonable results to draw a conclusive explanation.

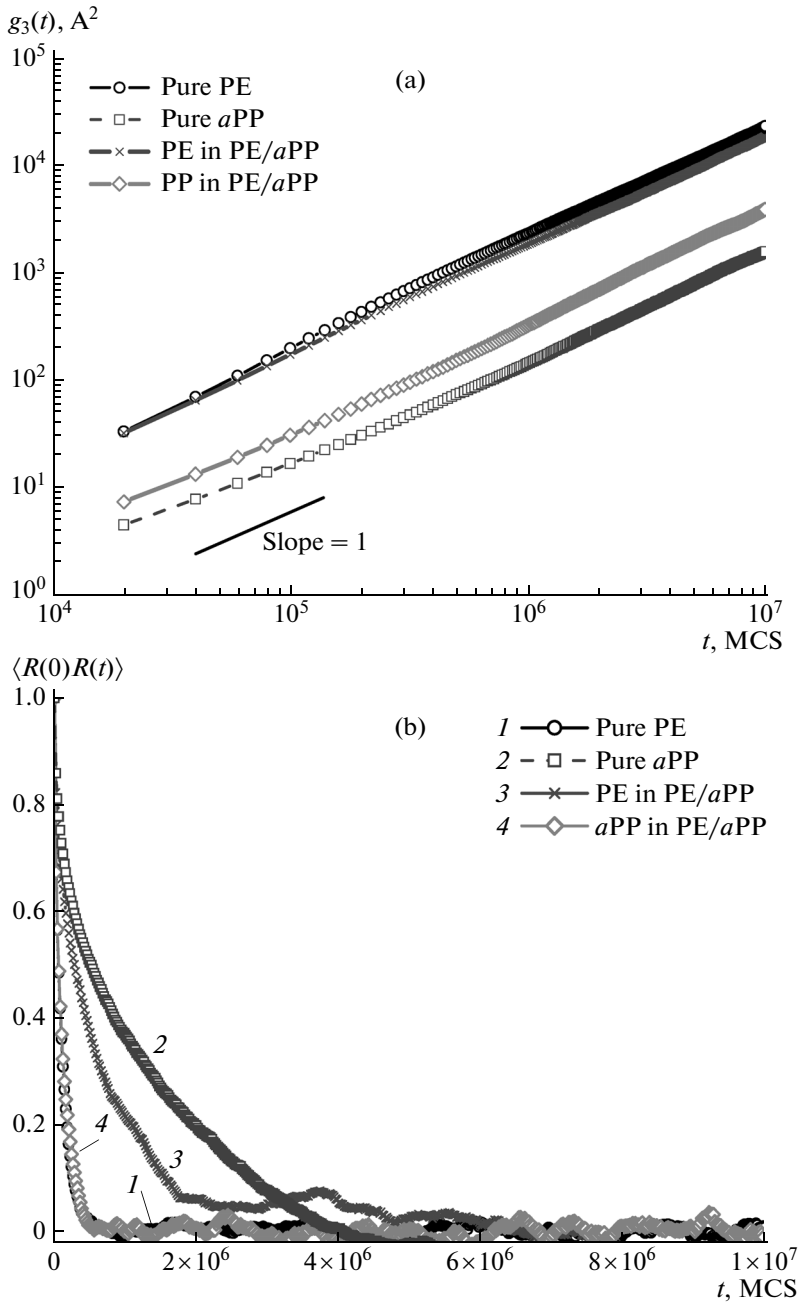

Fig. 1. (a) Typical mean square displacements of the chain center of mass (g_3) for neat PE and *a*PP melts and PE/*a*PP blend at 473 K. (b) Typical curves for the decay of the orientation auto-correlation function (OACF) of the end-to-end vectors of PE and *a*PP melt and PE/*a*PP blend at 473 K.

Structures and Dynamic Properties

The structures and dynamic properties of PE, *a*PP, *i*PP and *s*PP chains for neat melt and in blends are summarized in Table 2. The values in parentheses are the standard deviation of $\langle R_e^2 \rangle$ and $\langle R_g^2 \rangle$ which represent the statistical distribution of the molecular size. The dimension of PE chains (the mean square end-to-end distance, $\langle R_e^2 \rangle$, the characteristic ratio (C_n) and the mean square radius of gyration, $\langle R_g^2 \rangle$) in PE/PP blends is slightly decreased compared to neat PE melts and its decrease is obvious in PE/*s*PP system. The dimension of PE chains in the blends is weakly sensitive to the tacticity of PP. The molecular size is significantly increased for *a*PP and *i*PP in the blends whereas it is decreased for *s*PP compared to their neat PP melts. As the results, *a*PP and *i*PP chains tend to swell while *s*PP chains tend to shrink when they are

Table 2. Chain statistics of neat polymer melt and blends. The characteristic ratio (C_n), the mean square end-to-end distance, $\langle R_e^2 \rangle$, the radius of gyration, $\langle R_g^2 \rangle$, and self-diffusion coefficient, D, for PE, *a*PP, *i*PP and *s*PP chains are determined at 473 K. Chain dimensions are in unit of Å^2

Chain	Binary blend	C_n	$\langle R_e^2 \rangle$	$\langle R_g^2 \rangle$	$\langle R_e^2 \rangle/\langle R_g^2 \rangle$	D (Å/t) × 10^6
Neat PE	–	4.56	1045.02(781.97)	171.79(74.92)	6.08	2330.0
Neat *a*PP	–	4.53	1038.71(771.38)	169.84(73.38)	6.11	164.0
Neat *i*PP	–	4.41	1011.58 (745.61)	167.91(70.05)	6.02	206.2
Neat *s*PP	–	4.46	1024.35(841.19)	171.73(74.51)	5.96	3.82
PE	PE/*a*PP	4.63	1062.20(781.88)	172.38(74.85)	6.16	1890.0
PE	PE/*i*PP	4.46	1025.38(783.88)	169.70(74.31)	6.04	1760.0
PE	PE/*s*PP	4.52	976.05(770.23)	163.55(73.39)	5.97	1860.0
*a*PP	PE/*a*PP	4.75	1090.25(807.58)	181.36(74.34)	6.01	397.9
*i*PP	PE/*i*PP	5.19	1192.82(837.16)	190.14(76.27)	6.27	574.8
*s*PP	PE/*s*PP	3.94	904.05(727.97)	162.10(73.00)	5.58	7.0

The values in parentheses are standard deviation (S.D.) of $\langle R_e^2 \rangle$ and $\langle R_g^2 \rangle$.

blended with PE. Based on the change in molecular dimension, the demixing for *s*PP seems to be stronger than *a*PP and *i*PP in their blends with PE. The statistical distribution of $\langle R_e^2 \rangle$ and $\langle R_g^2 \rangle$ for PE is relatively unchanged in blends except for PE/*s*PP system. For *a*PP and *i*PP chains, the statistical distribution becomes broader in the blends except that of *s*PP chains which tend to narrower. A decrease in the width of statistical distribution of molecular size is related to demixing as polymer chains have to be confined within the segregated region as shown in Fig. 2.

When only the single bead move (no pivot move) is used, we can reasonably mimic the dynamics of polymer chains by mapping the Monte Carlo Step to the real time in comparison with molecular dynamic simulation or Pulse field gradient NMR experiment in term of the diffusion coefficient [22, 23]. Good agreement with those atomistic simulation and experiment allow us to use this Monte Carlo simulation with the local bead move to study, at least qualitatively, the dynamic characteristics of PE/PP blends.

The self-diffusion coefficients (D) of polymer molecules in pure melts and blends are also given in Table 2. The diffusion of PE chain in blends is slower compared to its neat melt. However, the values of D for PE chains in each blend systems are not much different and it is slightly sensitive to the tacticity of PP chains. In contrast to the diffusion behavior of PE molecules, the diffusion of PP chains can be ordered as *i*PP > *a*PP ⩾ *s*PP and are increased in the PE/PP blend compared to their neat PP melts. This behavior is quite different from results for chain dynamics from our recent simulation of PP/PP blends with different chain tactcity [21]. The diffusion rate of PP in PE/PP blends become faster after mixing. For PP/PP mixture with different tacticity [21], it was found that the mobility of PP chains is depended on both intramolecular (molecular size and chain stiffness) and intermolecular (chain packing) effects. In this work; however, an increased diffusion of PP chains in PE/PP blends should be more related to the chain packing as determined by the non-bonded shell interaction than the intramolecular contribution. The first two shell interaction that influence on the chain packing between PP and PP beads (26.693, 3.065, −1.088 kJ/mol) is higher than the interaction between PP and PE beads (18.401, 1.178, −0.879 kJ/mol). The decreased diffusion of PE chains in PE/PP blends should also be related to an increase of the chain packing as the interaction between PE and PE beads (12.980, 0.101, −0.593 kJ/mol) is lower than the interaction between PP and PE beads.

Pair Correlation Function

Figure 2 shows a cross section view of the representative snapshot for PE/*s*PP, PE/*a*PP and PE/*i*PP blends. By visual inspection, it can be clearly seen that *s*PP tend to demix with PE while *i*PP seems to be well dispersed in PE matrix. To quantitatively analysis the magnitude of the demixing in PE/PP blends, the pair correlation function for each system was calculated.

The pair correlation function (PCFs), $g_{AA}(r)$, used to describe the phase behavior of the mixtures, is often obtained from the probability of finding a particle A at a distance r from another particle A. Because the current study was performed on the discrete space, $g_{AA}(i)$ is defined based on the shell ith, instead of the usual definition based on a continuous distance, r. This dis-

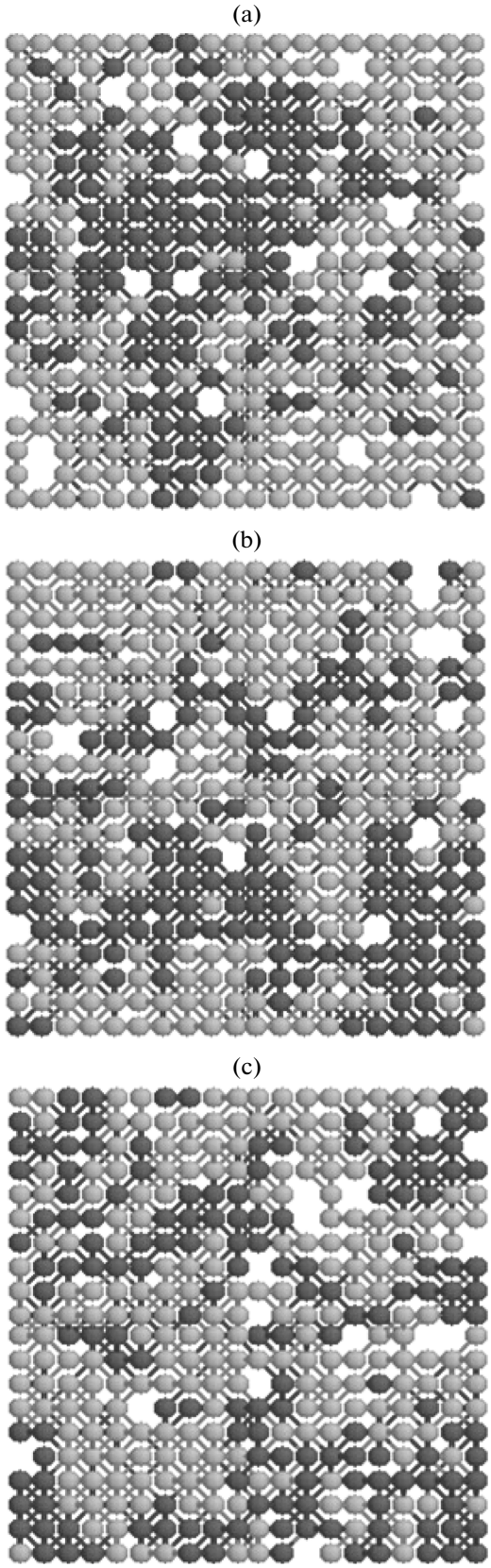

Fig. 2. A cross section view of the representative snapshot for (a) PE/*s*PP, (b) PE/*a*PP, and (c) PE/*i*PP blends (PE and PP beads are denoted by dark and light color, respectively).

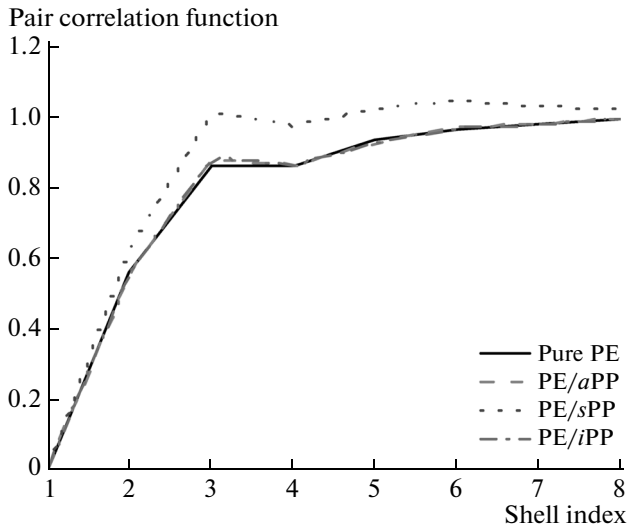

Fig. 3. Pair correlation functions, $g_{PE-PE}(i)$, for monomers of PE chains in the pure PE melt and PE/*a*PP, PE/*i*PP, and PE/*s*PP blends.

cretized form of the pair correlation function can be formulated as:

$$g_{AA}(i) = \frac{1}{(10i^2 + 2)V_A n_s}\sum n_{AA}(i), \qquad (4)$$

where V_A is the volume fraction of A in the system, n_s is the number of snapshots employed in the summation, and $n_{AA}(i)$ is the number occupancy of A in the *i*th shell from another A, where the two A's are from different chains. Thus the definition of $g_{AA}(i)$ is in terms of intermolecular pairs. The normalization is chosen so that $g_{AA}(i) = 1$ for a random distribution of particle [10].

Figure 3 shows the $g_{PE-PE}(i)$ curves of pure PE melt and PE chains in PE/*a*PP, PE/*i*PP and PE/*s*PP melt blends. The $g_{PE-PE}(i)$ curve in PE/*s*PP blends is the highest among the intermolecular PCFs. This indicates that PE monomers of each chain prefer to interact with another PE chains more than with any PP chains. In contrast, $g_{PE-PE}(i)$ curves in PE/*a*PP and PE/*i*PP blends are lower and almost the same as that of pure PE melts. These results suggest that the chain packing chracteristics for PE–*a*PP and PE–*i*PP pair are quite similar but it is more different for PE–*s*PP pair.

PCFs curves of PE/*a*PP, PE/*i*PP and PE/*s*PP mixtures are illustrated in Figs. 4, 5 and 6, respectively. The general features of PCFs curves of all blends show similar trends. The first and the largest well-defined peak occurs at the third shell. For each PE/PP blend, the PCFs curves for PE–PE pair, PP–PP pair and PE–PP pair are considered for comparison and discussion.

As shown in Fig. 4, the packing efficiency for the pure components, as assessed by the height of the first

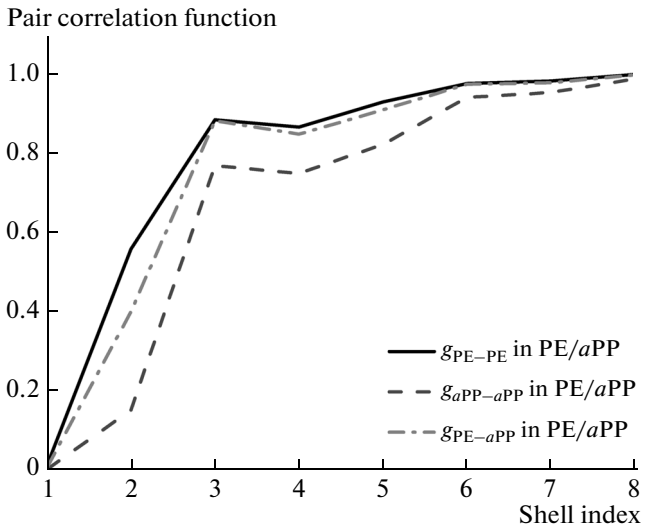

Fig. 4. Pair correlation functions, $g_{PE-PE}(i)$, $g_{aPP-aPP}(i)$, and $g_{PE-aPP}(i)$ for 50 : 50 by weight of PE/aPP blend.

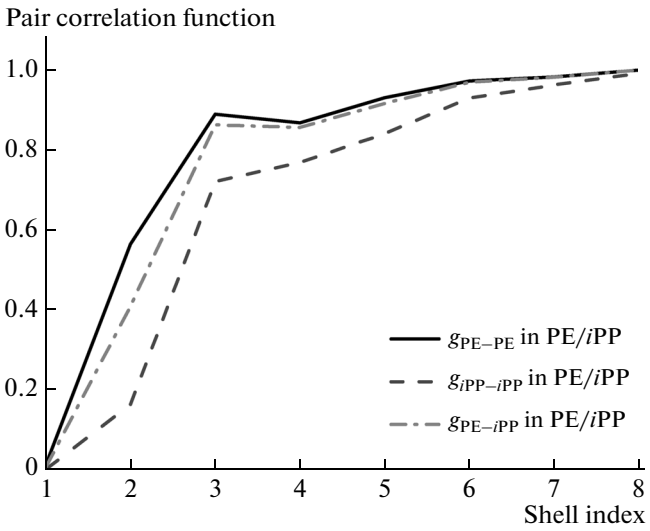

Fig. 5. Pair correlation functions, $g_{PE-PE}(i)$, $g_{iPP-iPP}(i)$, and $g_{PE-iPP}(i)$ for 50 : 50 by weight of PE/iPP blend.

peak in PCFs curves, follows the order as: PE–PE > PE–aPP ⩾ aPP–aPP. The g_{PE-aPP} curve is clearly distinguishable from the $g_{aPP-aPP}$ curve whereas it is weak different from the g_{PE-PE} curve. These results suggest that PE monomers can interact quite well with aPP monomer, which lead to weakly demix between PE and aPP in the blend. This observation also corresponds to a slightly increased chain dimension of PE and aPP in the blend compared to their neat melts.

For PE/iPP blend, the tendency of the PCFs curves is almost same to those in PE/aPP blend. However, the gap between g_{PE-iPP} and g_{PE-PE} curves is larger than the gap between g_{PE-aPP} and g_{PE-PE} curves as shown in Fig. 5. This implies that the demixing of PE/iPP is stronger than PE/aPP. This behavior is also consistent with results from the self-consistent polymer reference interaction site model (PRISM) calculations [7].

Figure 6 shows the PCFs curves of PE/sPP blend. It is evident that each PCFs curve is clearly distinguishable from each other, especially the highest peak at the third shell of $g_{sPP-sPP}$ curve, which imply that this blend has a strong tendency for phase separation. These results imply that PE/sPP mixtures should be the most probable to demix compared to PE/aPP and PE/iPP blends.

Energetics

The RIS states of the polymers can be monitored from the 2*nnd* simulation directly. After $2–3 \times 10^6$ MCS, the average populations in the three states, (t,g^+,g^-) appear to stabilize for most of the melts. The average *trans* fraction from simulation for each chains at 473 K are 0.695, 0.531, 0.604 and 0.686 for PE, iPP, aPP, and sPP, respectively. It is apparent that PE and sPP chain prefer *trans* conformation. The *trans* conformation should cause stiffer sPP chains and closer contact alignment and may lead to different energetics. However, the calculated solubility parameters for iPP, aPP, and sPP are 13.9 14.0, and 14.1 $(J/cm^3)^{1/2}$, respectively [9]. Only small difference in solubility parameters is found for each PP. In addition, an energy of mixing could be calculated for each of the blends and the average energy per bead in the two-component mixtures $(\Delta E_{mix}) = E_{AB} - (E_A + E_B)/2$. However, this process involves taking a small difference between two large numbers, and the uncertainties due to the fluctuations in each individual energy during the simulation accumulate to a larger value than ΔE_{mix} itself. For this

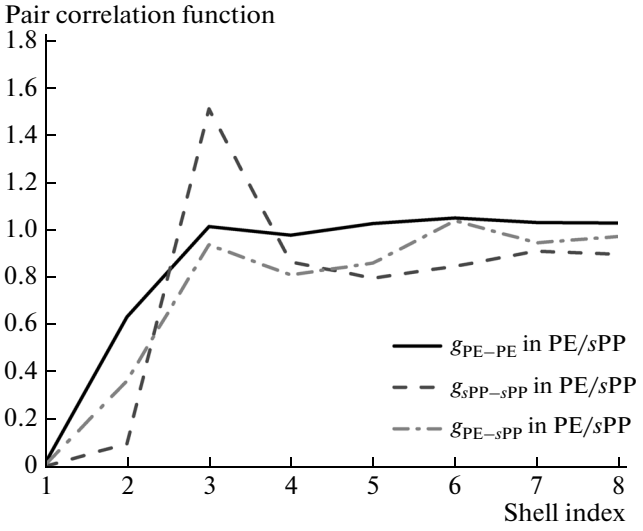

Fig. 6. Pair correlation functions, $g_{PE-PE}(i)$, $g_{sPP-sPP}(i)$, and $g_{PE-sPP}(i)$ for 50 : 50 by weight of PE/sPP blend.

reason, the energetic analysis of the blends to determine immiscibility is not investigated further here.

Discussion

For comparison, the molecular origin of the dependence of the mixing behavior of PP with PE chains in the melt was revealed by simulations of four one-component systems (PE, *i*PP, *a*PP, and *s*PP) and three 50 : 50 blends (PE/*i*PP, PE/*a*PE, and PE/*s*PP). An analysis of the equilibrated 50 : 50 blends was initially performed with the four potentially distinguishable intermolecular pair correlation functions: pcf(AA), pcf(BB), pcf(AB), and pcf(XX) (A and B denote the two distinguishable components, and X denotes A plus B) [8]. These four intermolecular pair correlation functions are not much difference for both PE/*i*PP and PE/*a*PE melt. However, if either *i*PE or *a*PE component of the melt is replaced by sPP, pcf(AB) has a smaller amplitude at short separations than the other three pair correlation functions, and this shows that *s*PP tends to avoid close contact with PE more than either *a*PP or *i*PP. This avoidance is stronger in PE/*i*PP blends than in PE/*a*PP blends. A detailed analysis of the simulations reveals the molecular mechanism that is responsible for the behavior of the PE/PP blends. The strongest tendency to demix was seen for PE/*s*PP blends. This is because the racemo dyads in *s*PP prefer *trans–trans* conformations more strongly than pairs of bonds in *i*PP and *a*PP which strongly avoid the *trans–trans* conformation. These conformational preferences are incorporated into the simulations because the coarse-grained chains are constrained by the rotational isomeric state (RIS) model. When two extended subchains in *s*PP are separated in parallel direction by a distance slightly larger than the size σ of the Lennard–Jones (LJ) potential. The favorable LJ interactions between the two segments produce an energetically favorable, or slightly sticky, intermolecular interaction controlled by the size of ε. The *s*PP and PE chain must sacrifice the ability to participate in these intermolecular interactions if it is transferred from its own melt into *i*PP and *a*PP melt because these chains avoid the extended conformation of their subchains. The tendency for *s*PP to stronger demix from PE than *i*PP or aPP (which contains meso dyads that avoid the *trans–trans* conformation) requires this attractive interaction.

CONCLUSIONS

The demixing behavior of the 50 : 50% by weight of PE ($C_{100}H_{202}$) and PP ($C_{150}H_{302}$) at the melt state were simulated by lattice Monte Carlo simulation of coarse-grained polymer model. PE/*a*PP, PE/*i*PP and PE/*s*PP blends were investigated and compared to their neat PE, *a*PP, *i*PP and *s*PP melts. The structure and dynamic properties were investigated by means of the mean square end-to-end distance, $\langle R_e^2 \rangle$, the mean square radius of gyration, $\langle R_g^2 \rangle$ and the self-diffusion coefficient (D) of PE, *a*PP, *i*PP and *s*PP melts and PE/PP blends. In comparison with the pure melt, the chain dimension as well as the diffusion of PE chains in PE/PP blends is quite sensitive to the stereochemistry of PP. In addition, the molecular dimension of PP was also changed after mixing with PE. Miscibility of the blend was quantified by various intermolecular pair correlation functions (PCFs). PCFs results suggest that PE is weakly demixed with *a*PP and *i*PP, while the phase separation of PE/*s*PP blend is apparently stronger. The onset of a tendency of PE chains to demix from PP chains is apparent in the pair correlation functions although no such conclusion can be drawn from an examination of energetic criteria.

ACKNOWLEDGMENTS

The financial support for this work by the Commission on Higher Education for supporting by grant fund under the program Strategic Scholarships for Frontier Research Network for the Ph. D. Program is gratefully acknowledged. All of this work was done at Suranaree University of Technology (SUT), Thailand. A.T. and V.V. would like to thank SUT-HPCC (SUT High Performance Computer Cluster) for computational resources. V.V. thanks the support by Material Chemistry Research Group and Advance Organic Materials Research Group. A.T. and V.V. have contributed to this work as 40 and 60%, respectively.

REFERENCES

1. *Polyolefin Blends,* Ed. by D. Nwabunma and T. Kyu (Wiley-Interscience, New York, 2007).
2. R. Krishnamoorti, W. W. Graessley, N. P. Balsara and D. J. Lohse, Macromolecules **27**, 3073 (1994).
3. W. W. Graessley, R. Krishnamoorti, N. P. Balsara, L. J. Fetters, D. J. Lohse, D. N. Schulz, and J. A. Sissano, Macromolecules **27**, 2574 (1994).
4. F. S. Bates, M. F. Schultz, J. H. Rosedale and K. Almdal, Macromolecules **25**, 5547 (1992).
5. K.S. Schweizer and J.G. Curro, *PRISM Theory of the Structure, Thermodynamics, and Phase Transitions of Polymer Liquids and Alloys, in Advances in Polymer Science* (Springer-Verlag, Berlin, 1994), Vol. 116.
6. H. M. Freschmidt, R. A. Shanks, G. Moad, and A. Uhlherr, J. Polym. Sci., Part B: Polym. Phys. **39**, 1803 (2001).
7. D. Heine, D. T. Wu, J. G. Curro, and G. S. Grest, J. Chem. Phys. **118**, 194 (2003).
8. T. C. Clancy, M. Putz, J. D. Weinhold, J. G. Curro, and W. L. Mattice, Macromolecules **33**, 9452 (2000).
9. T. Haliloglu and W. L. Mattice, J. Chem. Phys. **111**, 4327 (1999).
10. P. Choi and W. L. Mattice, J. Chem. Phys. **121**, 8647 (2004).

11. J. Baschnagel, K. Binder, P. Doruker, A. A. Gusev, O. Hahn, K. Kremer, W. L. Mattice, F. Muller-Plathe, M. Murat, W. Paul, S. Santos, U. W. Suter, and V. Tries, Adv. Polym. Sci. **152**, 41 (2000).

12. E. D. Akten and W. L. Mattice, Macromolecules **34**, 3389 (2001).

13. P. J. Flory, *Statistical Mechanics of Chain Molecules* (Wiley, New York, 1969).

14. W. L. Mattice and U. W. Suter, *Conformational Theory of Large Molecules. The Rotational Isomeric State Model in Macromolecular Systems* (Wiley, New York, 1994).

15. A. Abe, R. L. Jernigan, and P. J. Flory, J. Am. Chem. Soc. **88**, 631 (1966).

16. U. W. Suter, S. Pucci, and P. Pino, J. Am. Chem. Soc. **97**, 1018 (1975).

17. J. Cho and W. L. Mattice, Macromolecules **30**, 637 (1997).

18. R. C. Reid, J. M. Prausnitz, and B. E. Poling, *The Properties of Gases and Liquids* (McGraw-Hill, New York, 1987).

19. T. C. Clancy and W. L. Mattice, J. Chem. Phys. **112**, 10049 (2000).

20. N. Metropolis, A. N. Rosenbluth, M. N. Rosenbluth, A. H. Teller, and E. Teller, J. Chem. Phys. **21**, 1087 (1953).

21. T. Pinijmontree and V. Vao-soongnern, Chin. J. Polym. Sci. **32**, 640 (2014).

22. P. Doruker and W. L. Mattice, Macromol. Symp. **133**, 47 (1998).

23. N. Waheed, W. L. Mattice, and E. D. von Meerwall, Macromolecules **40**, 1504 (2007).